References

BATTERMAN, B. W. (1964). *Phys. Rev.* **134**, 1354–1356.
BECKER, P. (1977). *Acta Cryst* A**33**, 243–249.
BECKER, P. & COPPENS, P. (1974). *Acta Cryst.* A**30**, 129–147.
CHANDRASEKHAR, S. (1956). *Acta Cryst.* **9**, 954–956.
CHANDRASEKHAR, S., RAMASESHAN, S. & SINGH, A. (1969). *Acta Cryst.* A**25**, 140–142.
COOPER, M. J. & ROUSE, K. D. (1970). *Acta Cryst.* A**26**, 214–223.
COPPENS, P. & HAMILTON, W. C. (1970). *Acta Cryst.* A**26**, 71–83.
DARWIN, C. G. (1922). *Philos. Mag.* **43**, 800–829.
DENNE, W. A. (1972) *Acta Cryst.* A**28**, 192–201.
IZRAEL, A. & PETROFF, J. F. (1973). *Acta Cryst.* A**29**, 541–544.
KATAGAWA, T. & KATO, N. (1974). *Acta Cryst.* A**30**, 830–836.
KATO, N. (1976). *Acta Cryst.* A**32**, 453–466.
LAWRENCE, J. L. (1977). *Acta Cryst.* A**33**, 232–234.
MATHIESON, A. MCL. (1977). *Acta Cryst.* A**33**, 133–136.
PENNING, P. & POLDER, D. (1961). *Philips Res. Rep.* **16**, 419–440.
SCHNEIDER, J. R. (1977). *Acta Cryst.* A**33**, 235–243.
SEILER, P., DOBLER, M. & DUNITZ, J. D. (1974). *Acta Cryst.* B**30**, 2744–2745.
THORNLEY, F. R. & NELMES, R. J. (1974). *Acta Cryst.* A**30**, 748–757.
ZACHARIASEN, W. H. (1967). *Acta Cryst.* **23**, 558–564.

Acta Cryst. (1978) A**34**, 336–341

A Neutron Diffraction Study of the Wavelength Dependence of Extinction in UO_2

BY M. SAKATA,* M. J. COOPER, K. D. ROUSE AND B. T. M. WILLIS

*Materials Physics Division, AERE Harwell, Oxfordshire OX*11 0*RA, England*

(*Received* 7 *August* 1977; *accepted* 21 *October* 1977)

Neutron diffraction measurements have been carried out on a single crystal of UO_2 examined at four different wavelengths; 0·85, 1·12, 1·54 and 1·84 Å. The Bragg intensities were analysed for the wavelength dependence of extinction using both the Cooper–Rouse and the Becker–Coppens formulations. Both treatments showed that the crystal is of type I (*i.e.* $r \gg \lambda g$, where r is the domain radius, λ the wavelength and g the mosaic-spread parameter). The value of g is the same, within one standard deviation, for each wavelength; its magnitude is appreciably less than for other crystals (SrF_2,ZnS,ZnTe,KCl) which have been examined by neutron diffraction at a number of wavelengths. Keeping the isotropic temperature factor for uranium fixed at 0·28 Å^2, the value of 0·55 ± 0·02 Å^2 is derived for the temperature factor of oxygen. There are no significant differences between the values of the extinction parameters and temperature factors obtained using the Cooper–Rouse treatment and the Becker–Coppens treatment based on either a Gaussian or a Lorentzian mosaic-spread distribution.

1. Introduction

Currently there is much interest in measuring neutron Bragg intensities using a fixed scattering angle 2θ and a variable wavelength λ. Pulsed sources such as the Harwell LINAC adopt this arrangement instead of the more conventional system with a variable scattering angle and fixed wavelength. It is, therefore, of much interest to examine extinction effects as a function of wavelength. In this paper we report measurements of the neutron Bragg intensities of a single crystal of UO_2 at four different wavelengths: 0·85, 1·12, 1·54 and 1·84 Å. The measurements have been analysed using two theories of extinction: those due to Cooper & Rouse (1970) and Becker & Coppens (1974*a*,*b*, 1975). We show that, for this sample, the two theories give essentially the same results and cannot, therefore, be distinguished from one another. To distinguish the two theories requires measurements carried out on a crystal with larger secondary extinction than the UO_2 crystal, or on a crystal in which the extinction is determined by the domain radius rather than the mosaic spread (a type II crystal).

2. Cooper–Rouse theory

The Cooper–Rouse theory is based on that of Zachariasen (1967). The Zachariasen treatment of

---

* On leave from Nagoya University, Nagoya, Japan.

secondary extinction can be summarized in the equations:

$$F_c^2 = F_k^2 y, \tag{1}$$

$$y = (1+2x)^{-1/2}, \tag{2}$$

$$x = r^* Q \lambda^{-1} \bar{T}, \tag{3}$$

$$r^* = \frac{r}{[1+(r/\lambda g)^2]^{1/2}}. \tag{4}$$

Here F_c is the calculated extinguished structure factor, F_k is the kinematical structure factor, y is the extinction factor, r is the domain radius, g is the mosaic-spread parameter, Q is the conventional crystallographic quantity proportional to $F^2\lambda^3$ cosec 2θ, and $\bar{T}$ is the mean path length through the crystal.

Cooper & Rouse replace (2) by a function

$$y = f(x, \sin\theta), \tag{5}$$

to allow for the θ dependence of the effective path length in the crystal. f was chosen for both spherical and cylindrical crystals to give the observed form of the extinction measured in CaF_2 and SrF_2 at three wavelengths.

Zachariasen distinguishes two types of crystal, depending on the relative magnitudes of r and λg. For type I crystals, $r \gg \lambda g$ and the extinction is determined by the mosaic-spread parameter g. For type II crystals, $r \ll \lambda g$ and $r^* = r$, so that the extinction is determined by the domain radius r.

3. Becker–Coppens theory

Becker & Coppens (1974*a*) (BC) have derived a more rigorous theory of extinction which is valid for spherical crystals. The domain radius r in the Cooper–Rouse (CR) theory is replaced by $r \sin 2\theta$ in the BC theory. BC also derive expressions for both a Gaussian and a Lorentzian distribution of the mosaic spread parameter. These expressions are:

$$F_c^2 = F_k^2 y_s \tag{6}$$

$$y_s = f(x, \sin\theta) \tag{7}$$

$$x = r^*(\sin 2\theta) Q \lambda^{-1} \bar{T} \tag{8}$$

where r^* for a Gaussian distribution is

$$r_G^* = \frac{r}{\{1+\frac{9}{8}[r(\sin 2\theta)/\lambda g]^2\}^{1/2}}. \tag{9}$$

and r^* for a Lorentzian distribution is

$$r_L^* = \frac{r}{1+[r(\sin 2\theta)/\lambda g]}. \tag{10}$$

For type I crystals: $r \gg \lambda g$ and so

$$\left.\begin{aligned} r_G^* &= \tfrac{8}{9}\lambda g/\sin 2\theta, \\ \text{and} \qquad x_G &= \tfrac{8}{9} g Q \bar{T}; \end{aligned}\right\} \tag{11}$$

$$\left.\begin{aligned} r_L^* &= \lambda g/\sin 2\theta \\ \text{and} \qquad x_L &= g Q \bar{T}. \end{aligned}\right\} \tag{12}$$

For type II crystals $r \ll \lambda g$ and so

$$\left.\begin{aligned} r_G^* &= r_L^* = r \\ \text{and} \qquad x_G &= x_L = r(\sin 2\theta) Q \lambda^{-1} \bar{T}. \end{aligned}\right\} \tag{13}$$

For spherical crystals of type I the BC and CR formulations for secondary extinction are identical except for the exact form of the function $f(x, \sin\theta)$.

Primary extinction is included by replacing (6) with

$$F_c^2 = F_k^2 y_s y_p, \tag{14}$$

where y_p has a similar form to y_s, (7), but with x given by

$$x_p = \tfrac{3}{2} Q r^2 (\sin 2\theta)/\lambda. \tag{15}$$

4. Experimental

The crystal, which was vapour grown, was supplied by the late Dr Van Lierde of Mol Donc, Belgium, and was ground to a sphere of 1 mm radius in a modified Bond grinder (Arndt & Willis, 1966). Detailed study of neutron diffraction profiles before and after grinding indicated a Gaussian mosaic-spread distribution and no evidence of effects due to surface damage was observed.

The spherical crystal was mounted on the Mark 6 Harwell four-circle diffractometer. Bragg intensity data were collected at 0·85, 1·12, 1·54 and 1·84 Å, and were derived by averaging intensity measurements over four equivalent diffracting planes. The different wavelengths were obtained by choosing different reflecting planes of a Ge monochromator.

Some anisotropy in the extinction was observed, particularly for the strongest reflections and the longest wavelengths. However, averaging of the data over equivalent reflections enabled an isotropic model for the extinction to be used.

5. Data analysis

The data sets were analysed by the Harwell *TAILS* computer program. The program determines those values of the variable parameters which minimize the quantity

$$S = \sum_i w_i (I_{oi} - I_{ci})^2, \tag{16}$$

where I_{oi} is the observed intensity, I_{ci} is the corresponding calculated intensity and w_i is the weight of the observation. I_c is given by

$$I_c = sA_\mu(y+\alpha)|F_c|^2 \operatorname{cosec} 2\theta \qquad (17)$$

where s is the scale factor, A_μ the absorption factor, y the extinction factor and α the correction due to thermal diffuse scattering. A_μ for a spherical crystal is tabulated by Rouse, Cooper, York & Chakera (1970). α is calculated using the isotropic approximation of Cooper & Rouse (1968). Because of correlation with other parameters, especially at long wavelengths, the temperature-factor of uranium was fixed at 0·28 Å^2 throughout the analysis. This value has been obtained recently by Rouse & Willis (1977) using powder diffraction. The third-order anharmonic parameter associated with the vibration of the oxygen atoms was also fixed at the value given by Rouse, Willis & Pryor (1968). The scattering length ratio b_U/b_O was fixed at 1·426, which was determined by a reanalysis of the data obtained by Rouse, Willis & Pryor (1968).

In all cases the data for different wavelengths were analysed separately, in order to ensure that wavelength-dependent effects were not concealed.

(*a*) *Cooper–Rouse theory*

The effective domain radius r^* was derived at each wavelength using the theory in § 2, and the results are summarized in Table 1. The value of r^* can be obtained without knowing whether the crystal is of type I or type II [see equation (13)].

Table 1. *The results of Cooper & Rouse analyses for* UO_2 *refining the effective domain radius* r^*

	λ(Å)	$y_{\min}$	r^* (10^{-5} cm)	R(%)
UO_2 (sphere)	0·85	0·77	0·46 (8)	1·8
	1·12	0·67	0·60 (8)	2·1
	1·54	0·52	0·85 (15)	3·5
	1·84	0·42	1·17 (22)	2·8

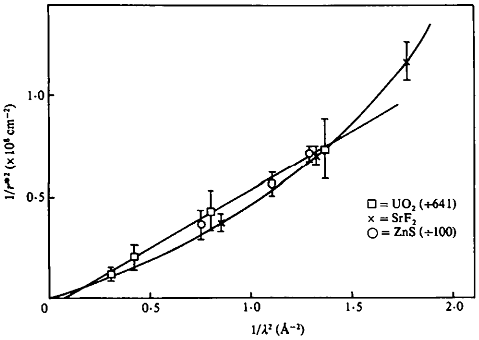

Fig. 1. Plot of $1/r^{*2}$ against $1/\lambda^2$ for UO_2. The figure also includes the previous results of SrF_2 and ZnS which have been derived by two of the present authors (Cooper & Rouse, 1976). For convenience the values of $1/r^{*2}$ for UO_2 have been divided by 641 to bring them on to the same scale as those for SrF_2. Similarly those for ZnS have been divided by 100.

Writing (4) in the form

$$\frac{1}{r^{*2}} = \frac{1}{r^2} + \frac{1}{(\lambda g)^2} \qquad (18)$$

we can determine r and g by plotting $1/r^{*2}$ *versus* $1/\lambda^2$. However, the resultant curve, Fig. 1, has a negative intercept on the $1/r^{*2}$ axis, so that this implies that (18) is not strictly true. This deficiency in the theory has been noted already by Cooper & Rouse (1976). We conclude that the intercept on the $1/r^{*2}$ axis is very small. Assuming that the intercept is zero, the g value in (18) works out at 0·55 (0·04) × 10^3 rad^{-1}. For comparison, this figure includes the results given by Cooper & Rouse (1976) for SrF_2 and ZnS with the values of $1/r^{*2}$ for UO_2 and ZnS divided by 641 and 100 respectively to bring them on to the same scale as those for SrF_2.

Table 2 summarizes the values of the parameters given by the CR treatment with the value of B_U fixed at 0·28 Å^2. We note that B_O is the same, within one standard deviation, for all four wavelengths. g is the mosaic-spread parameter and the R values vary between 1·8 and 3·5% for the different wavelengths. Clearly, the crystal is of Zachariasen's (1967) type I, for which $r \gg \lambda g$ [see equation (11)].

(*b*) *Becker–Coppens theory*

There are a number of alternative models for the BC theory. Thus the mosaic spread may be represented by either a Gaussian or a Lorentzian function, and the crystal may be of type I [equations (11) and (12)] or type II [equation (13)].

In Table 3 we give for the type II, BC theory the same parameters as in Table 2 for the CR theory.

Table 2. *Results of Cooper & Rouse analyses of* UO_2 *data*

	λ_1(0·85 Å)	λ_2(1·12 Å)	λ_3(1·54 Å)	λ_4(1·84 Å)
B_O (Å^2)	0·56 (2)	0·55 (1)	0·59 (6)	0·55 (5)
$r \times 10^5$ (cm)	–	–	–	–
$g \times 10^{-3}$	0·54 (7)	0·54 (7)	0·55 (9)	0·63 (12)
R (%)	1·8	2·1	3·5	2·7
wR (%)	3·9	2·4	3·6	3·6

Table 3. *Results of Becker & Coppens analyses of* UO_2 *data: type* II

	λ_1	λ_2	λ_3	λ_4
B_O (Å^2)	0·55 (3)	0·55 (2)	0·56 (5)	0·49 (6)
$r \times 10^5$ (cm)	0·57 (11)	0·68 (11)	0·85 (13)	0·92 (33)
$g \times 10^{-3}$	–	–	–	–
R (%)	4·6	4·6	3·3	5·1
wR (%)	4·9	2·9	4·1	3·9

Table 4 refers to type I, BC theory, assuming a Gaussian mosaic spread. Table 5 gives results obtained for the type I, BC theory assuming a Lorentzian mosaic spread. Comparing Tables 3 and 4, we note that the *R* factor is appreciably lower for Table 4, and conclude that the crystal is of type I, as previously concluded from the CR analysis [§ 5 (*a*)]. The analysis based on a Lorentzian distribution gives slightly higher values of *R* and *wR* than the analysis of the type I Gaussian distribution. The Gaussian analysis is, therefore, to be preferred to the Lorentzian analysis in contrast to the results obtained previously for SrF_2 (Cooper & Rouse, 1976).

In order to investigate further the crystal type, we used a mixed type of analysis with both *r* and *g* refined. The results are shown in Table 6. In the table *g* is accurately determined but *r* is not (the standard deviation of *r* is appreciably larger than *r* itself). This means that in this case the effective domain radius r^* is determined by the mosaic spread. *R* and *wR* are not appreciably different from the values in Table 4 for type I Gaussian distribution. Thus we confirm once more that the crystal is of type I.

We have also analysed the data using the BC theory assuming primary extinction alone, see Table 7. Comparing the *R* factors in this table with those in Table 4 shows that the primary extinction is less significant than secondary extinction.

Finally, in Table 8 we refine both primary and secondary extinction parameters on the BC theory, equation (14). Comparison of Tables 4 and 8 shows, once more, that secondary extinction is dominant. It should be noted that in Table 8, *g* is not accurately determined, its standard deviations being much larger than in the earlier models. This arises from the correlation between B_O and *g*: see last row of Table 8.

Table 4. *Results of Becker & Coppens analyses of* UO_2 *data: type* I *Gaussian mosaic spread*

	λ_1	λ_2	λ_3	λ_4
B_O (Å^2)	0·56 (2)	0·55 (2)	0·59 (5)	0·52 (4)
$r \times 10^{-5}$ (cm)	–	–	–	–
$g \times 10^{-3}$	0·55 (7)	0·50 (6)	0·51 (7)	0·51 (7)
R (%)	1·4	1·9	3·6	1·0
wR (%)	3·9	2·6	3·6	3·3

Table 5. *Results of Becker & Coppens analyses of* UO_2 *data: type* I *Lorentzian mosaic spread*

	λ_1	λ_2	λ_3	λ_4
B_O (Å^2)	0·56 (2)	0·56 (1)	0·60 (5)	0·56 (5)
$r \times 10^5$ (cm)	–	–	–	–
$g \times 10^{-3}$	0·58 (6)	0·55 (8)	0·62 (11)	0·69 (15)
R (%)	1·7	2·3	3·0	3·0
wR (%)	4·0	2·8	3·8	3·8

Table 6. *Results of Becker & Coppens analyses of* UO_2 *data: type* I + *type* II *Gaussian mosaic spread*

	λ_1	λ_2	λ_3	λ_4
B_O (Å^2)	0·56 (1)	0·54 (1)	0·57 (4)	0·51 (4)
$r \times 10^5$ (cm)	65 (13500)	2·2 (166)	1·6 (6)	42 (6520)
$g \times 10^{-3}$	0·50 (2)	0·52 (8)	0·64 (13)	0·51 (11)
R (%)	1·8	2·0	2·7	1·2
wR (%)	3·8	2·5	3·4	3·3

Table 7. *Results of Becker & Coppens analyses of* UO_2 *data: primary extinction only*

	λ_1	λ_2	λ_3	λ_4
B_O (Å^2)	0·55 (3)	0·54 (2)	0·57 (5)	0·49 (10)
$r \times 10^5$ (cm)	81 (9)	88 (9)	107 (10)	119 (26)
$g \times 10^{-3}$	–	–	–	–
R (%)	4·8	5·4	3·6	5·4
wR (%)	5·0	2·8	4·3	4·2

Table 8. *Results of Becker & Coppens analyses of* UO_2 *data: primary and secondary extinction; Gaussian mosaic spread*

Correlation represents the element of the correlation matrix between B_O and $1/g$.

	λ_1	λ_2	λ_3	λ_4
B_O (Å^2)	0·57 (2)	0·54 (1)	0·55 (4)	0·51 (5)
$r \times 10^5$ (cm)	9·5 (220)	26 (22)	61 (19)	16 (52)
$g \times 10^{-3}$	0·53 (40)	0·45 (22)	0·26 (11)	0·49 (17)
R (%)	1·5	1·9	2·4	0·7
wR (%)	3·8	2·4	3·0	3·3
Correlation	0·98	0·95	0·93	0·89

Table 9. *Neutron diffraction data for* UO_2 *at* $\lambda = 0{\cdot}85$ Å

h k l	I_o	I_c	$\sigma(I_o)$	y	α
2 2 0	11091	11280	262	0·772	0·002
4 0 0	8231	8318	82	0·830	0·004
4 2 2	6904	6847	69	0·860	0·007
4 4 0	5798	5911	71	0·880	0·010
6 2 0	5354	5241	54	0·893	0·013
4 4 4	4830	4737	54	0·904	0·017
2 0 0	488	553	14	0·988	0·001
2 2 2	258	278	11	0·994	0·003
4 2 0	158	185	8	0·996	0·006
6 0 0	97	100	4	0·998	0·012
4 4 2	94	100	6	0·998	0·012
6 2 2	92	76	5	0·998	0·015
1 1 1	3832	3897	38	0·918	0·001
3 1 1	2093	2100	21	0·956	0·003
3 3 1	1605	1597	16	0·966	0·005
3 3 3	1353	1354	14	0·972	0·008
5 1 1	1353	1341	18	0·972	0·008
5 3 1	1200	1184	12	0·975	0·011
5 3 3	1095	1050	3	0·978	0·015
5 5 1	1006	971	3	0·980	0·018

The primary-plus-secondary extinction formulation of Becker & Coppens represents the most general treatment of extinction amongst many alternative models of this theory.

The experimental data are summarized in Tables 9 to 12. These tables list the observed and calculated background-corrected intensities, the standard deviations of the observed intensities based on counting statistics, and the values of the extinction and thermal diffuse scattering factors for each reflection. The calculated intensities and extinction factors are those obtained using the Cooper–Rouse formulation.

Table 10. *Neutron diffraction data for* UO_2 *at* $\lambda = 1{\cdot}12$ Å

$h\,k\,l$	I_o	I_c	$\sigma(I_o)$	y	α
2 2 0	15490	15736	270	0·668	0·001
4 0 0	12100	12241	192	0·740	0·004
4 2 2	10487	10476	213	0·777	0·006
4 4 0	8756	9386	190	0·800	0·008
6 2 0	8747	8673	87	0·817	0·011
2 0 0	805	877	12	0·980	0·001
2 2 2	433	455	6	0·990	0·002
4 2 0	334	314	16	0·993	0·005
6 0 0	188	184	6	0·996	0·009
4 4 2	184	184	3	0·996	0·009
6 2 2	153	148	4	0·997	0·012
1 1 1	6023	5864	60	0·868	0·000
3 1 1	3330	3298	33	0·925	0·002
3 3 1	2548	2584	25	0·942	0·004
3 3 3	2280	2252	23	0·949	0·007
5 1 1	2263	2232	46	0·949	0·007
5 3 1	2054	2036	21	0·954	0·009
5 3 3	1960	1879	22	0·958	0·011

Table 11. *Neutron diffraction data for* UO_2 *at* $\lambda = 1{\cdot}54$ Å

$h\,k\,l$	I_o	I_c	$\sigma(I_o)$	y	α
2 2 0	21109	21106	730	0·522	0·001
4 0 0	17522	17831	473	0·596	0·003
4 2 2	15764	16610	347	0·631	0·005
4 4 0	14990	16549	300	0·643	0·006
2 0 0	1359	1434	15	0·961	0·001
2 2 2	769	771	19	0·979	0·002
4 2 0	598	556	13	0·985	0·004
1 1 1	9206	8750	92	0·774	0·000
3 1 1	5443	5382	54	0·860	0·002
3 3 1	4641	4521	46	0·882	0·004
3 3 3	4308	4320	45	0·888	0·005
5 1 1	4258	4277	43	0·888	0·005

Table 12. *Neutron diffraction data for* UO_2 *at* $\lambda = 1{\cdot}84$ Å

$h\,k\,l$	I_o	I_c	$\sigma(I_o)$	y	α
2 2 0	26745	27882	1034	0·416	0·001
4 0 0	24924	25753	663	0·484	0·003
2 0 0	2282	2277	66	0·936	0·000
2 2 2	1279	1329	17	0·963	0·002
4 2 0	1158	1077	25	0·970	0·003
1 1 1	12375	12331	174	0·679	0·000
3 1 1	8281	8263	119	0·783	0·002
3 3 1	7677	7564	77	0·805	0·003

(*c*) *Comparison of Cooper–Rouse and Becker–Coppens treatments*

Table 4 is the most appropriate table for the BC analysis for comparison with the CR results of Table 2. The weighted R factors are very similar in the two tables, even for the extreme case of the longest wavelength ($\lambda = 1{\cdot}84$ Å). For this reason we cannot usefully distinguish between the two theories. This is because the BC and CR expressions have exactly the same form for type I crystals, except for the function $f(x, \sin\theta)$.

Fig. 2 illustrates the determination of the value of B_O, as derived at different wavelengths and for different extinction treatments. Its value is remarkably constant for these different conditions and its mean value is $0{\cdot}555 \pm 0{\cdot}012$ Å^2. It does not matter which extinction theory is used from the viewpoint of determining the crystallographic quantity B_O, which relates to the isotropic amplitude of motion of the O atom. This seems consistent with the results of yttrium iron garnet obtained by Bonnet, Delapalme, Fuess & Thomas (1975) in which both the Zachariasen theory and the BC theory were used but no significant differences were observed in the crystallographic parameters obtained using the various extinction models.

6. Conclusions

We have examined a small spherical crystal of UO_2 at four different wavelengths between 0·85 and 1·84 Å, and have analysed the results using both the Cooper–Rouse and Becker–Coppens theories of extinction. Both theories lead to the same conclusions and so we cannot say in this case whether one theory is preferable to another. The nature of the extinction in the UO_2 crystal is type I secondary (*i.e.* $r \gg \lambda g$, where r is the domain radius, λ the wavelength and g the mosaic-

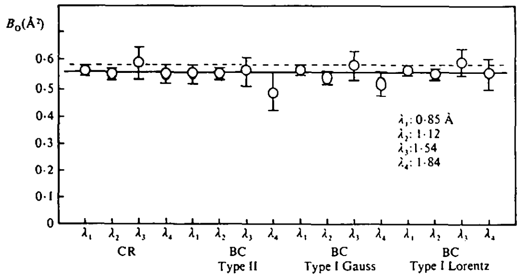

Fig. 2. Plot of the temperature factor *versus* wavelength for different extinction theories. The full line represents the average value of B_O and the broken line represents the value determined by powder diffraction (Rouse & Willis, 1977).

spread parameter). Of the two distributions, Gaussian and Lorentzian, which can be used for describing the mosaic spread in the Becker–Coppens theory, the Gaussian distribution gives slightly lower R factors and is therefore to be preferred. The isotropic temperature factor of the O atom refines at $0{\cdot}55 \pm 0{\cdot}02$ Å^2 when the temperature factor of the U atom is kept fixed at the value, $0{\cdot}28$ Å^2, derived from powder data. The magnitude of the temperature factor is the same whatever version of the extinction theory is used. The most general form of the Becker–Coppens theory includes both primary and secondary extinction, but this form is not particularly useful because of the very high correlation between the temperature factor $B_{\rm O}$ and the extinction parameter g.

The results of this analysis are consistent with the conclusion of Cooper & Rouse (1976) that the extinction theories do not account adequately for the wavelength dependence of the extinction. However, the extinction in the UO_2 crystal was not sufficiently large for the additional variation with wavelength to be significant in this case.

These results confirm that the values derived for the temperature factors in this type of material are dependent on the correction for extinction, but are insensitive to the exact model which is used for this. In type I crystals, for which the extinction is determined by the mosaic spread of the sample, the Cooper–Rouse and Becker–Coppens theories both provide an adequate model for the extinction properties, even for effects approaching a 60 % reduction in intensity. We may therefore conclude that, in general, if extinction effects are significant reliable values of the temperature factors will not be obtained unless an extinction correction is applied, but that the choice of model is not important for type I crystals. However, analysis of data collected at different wavelengths may conceal inadequacies in the wavelength dependence of the models, unless the various sets of data are analysed separately.

References

Arndt, U. W. & Willis, B. T. M. (1966). *Single Crystal Diffractometry*, pp. 257–258. Cambridge Univ. Press.

Becker, P. J. & Coppens, P. (1974*a*). *Acta Cryst.* **A30**, 129–147.

Becker, P. J. & Coppens, P. (1974*b*). *Acta Cryst.* **A30**, 148–153.

Becker, P. J. & Coppens, P. (1975). *Acta Cryst.* **A31**, 417–425.

Bonnet, M., Delapalme, A., Fuess, H. & Thomas, M. (1975). *Acta Cryst.* **B31**, 2233–2240.

Cooper, M. J. & Rouse, K. D. (1968). *Acta Cryst.* **A24**, 405–410.

Cooper, M. J. & Rouse, K. D. (1970). *Acta Cryst.* **A26**, 214–223.

Cooper, M. J. & Rouse, K. D. (1976). *Acta Cryst.* **A32**, 806–812.

Rouse, K. D., Cooper, M. J., York, E. J. & Chakera, A. (1970). *Acta Cryst.* **A26**, 682–691.

Rouse, K. D. & Willis, B. T. M. (1977). Private communication.

Rouse, K. D., Willis, B. T. M. & Pryor, A. W. (1968). *Acta Cryst.* **B24**, 117–122.

Zachariasen, W. H. (1967). *Acta Cryst.* **23**, 558–564.

SHORT COMMUNICATIONS

Contributions intended for publication under this heading should be expressly so marked; they should not exceed about 1000 *words; they should be forwarded in the usual way to the appropriate Co-editor; they will be published as speedily as possible.*

Acta Cryst. (1978). A**34**, 341–343

Fourier transforms of Gaussian orbital products.

By G. S. Chandler and M. A. Spackman, *The School of Chemistry, University of Western Australia, Nedlands, WA* 6009, *Australia*

(*Received* 16 *August* 1977; *accepted* 29 *September* 1977)

An expression for the Fourier transform of two-centre Gaussian orbital products is obtained which is identical in form with expressions for overlap integrals. The one-centre transform is a special case, and is obtained in a trivial way from the two-centre expression. Explicit expressions of the transform for all combinations up to *ff* products are given.

Introduction

Recently, the calculation of X-ray structure factors from molecular wave-functions has attracted considerable interest (Bentley & Stewart, 1974, 1975; Groenewegen & Feil, 1969; McWeeny, 1953; Stevens, Rys & Coppens, 1977; Stewart, 1969). In the framework of molecular-orbital theory this calculation requires the evaluation of the Fourier transforms of atomic-orbital products;

$$X_{\mu\nu}(\mathbf{S},\mathbf{R}) = \int \chi_\mu^* \chi_\nu \exp(i\mathbf{S}\cdot\mathbf{r})\,\mathrm{d}\mathbf{r}. \qquad (1)$$